

Covalently bonded dendrimer-maghemite nanosystems: nonviral vectors for *in vitro* gene magnetofection†Blanca González,<sup>ac</sup> Eduardo Ruiz-Hernández,<sup>ac</sup> María José Feito,<sup>b</sup> Carlos López de Laorden,<sup>ac</sup> Daniel Arcos,<sup>ac</sup> Cecilia Ramírez-Santillán,<sup>b</sup> Concepción Matesanz,<sup>b</sup> María Teresa Portolés<sup>b</sup> and María Vallet-Regí<sup>\*ac</sup>

Received 18th October 2010, Accepted 4th January 2011

DOI: 10.1039/c0jm03526b

In this work novel nonviral nanosystems for *in vitro* gene magnetofection are presented. The multifunctional vectors consist of superparamagnetic iron oxide nanoparticles functionalized with low generations of poly(propyleneimine) dendrimers. The dendrimers are attached to the iron oxide nanoparticles through covalent bonds *via* a one-pot sol-gel synthetic route. This approach allows a direct dendritic decoration of the iron oxide NPs without any additional surface modification. Furthermore, this strategy avoids the multistep procedures of dendritic growth onto solid surfaces. The core-shell hybrid structures are water soluble as colloidal ferrofluids which are long-term stable at physiological pH. *In vitro* transfection experiments were assayed with Saos-2 osteoblasts, using as reporter gene a plasmid DNA that codes for the green fluorescent protein. Gene delivery experiments were carried out in the presence and in the absence of a magnetic field. The transfection efficiency strongly depends on the presence of the magnetic field and the dendrimer generation. The covalent bonding between the dendrimers and the magnetic nanoparticles surface ensures the vector integrity throughout storage and application. The nanosystems couple the DNA fragments and safely transport them under magnetic stimulus from the extracellular environment to the interior of the cell.

## Introduction

Gene transfection represents an alternative or complementary therapy in the treatment of cancer and other gene-based diseases.<sup>1,2</sup> This strategy consists of deliberately introducing nucleic acids into the nucleus of cells. In terms of gene therapy, the incorporation of nucleic acids is mainly intended to replace deleterious mutant alleles with functional ones, or even to induce the malignant cell apoptosis. Moreover, the DNA reprogramming of bacteria and eukaryotic cells opens huge possibilities in the field of biotechnology.<sup>3-5</sup>

The use of nonviral vectors is one of the main strategies for gene delivery into the target cell nucleus. These nanosystems induce minimal host immune responses and they have been increasingly proposed as a safer alternative to viral vectors. In

order to improve the efficiency of the gene transfer, a nonviral vector should fulfill the following requirements:<sup>6-8</sup>

(i) capability to complex nucleic acids and protect them against serum nuclease enzymes at the extracellular compartment, (ii) exhibit positive net electric surface charge at physiological pH to overcome the negative potential of the cell membrane, since otherwise the cell membrane impedes the incorporation of negatively charged phosphate-containing DNA, (iii) possess a mechanism to protect DNA from the acid environment inside endosomes and (iv) chemical stability to maintain the integrity until reaching the nucleus. Furthermore, by means of preparing multifunctional vectors, transfection can be accelerated thus hindering the biochemical attack over the gene. In this sense, magnetofection is an excellent alternative to significantly reduce the transfection time from several hours to less than 60 min. The association of superparamagnetic nanoparticles (NPs) with gene vectors makes possible to assist the transfection into cells by the application of an external magnetic field, which targets and reduces the duration of the gene delivery, enhancing the efficiency of the DNA vector.<sup>9</sup> In this sense, the coating of superparamagnetic iron oxide NPs with polycationic polymers such as polyethyleneimine makes magnetofection feasible.<sup>10-12</sup>

Dendrimers are tree-like highly branched macromolecules that possess unique three-dimensional architectures. Their features include a monodisperse polymeric constitution, well-defined internal cavities, nanometric dimensions, and the presence of a large number of functionalities on the surface.<sup>13</sup> Dendrimers

<sup>a</sup>Departamento de Química Inorgánica y Bioinorgánica, Facultad de Farmacia, Universidad Complutense de Madrid, Plaza de Ramón y Cajal s/n, 28040 Madrid, Spain. E-mail: vallet@farm.ucm.es; Fax: +34 91 3941786; Tel: +34 91 3941843

<sup>b</sup>Departamento de Bioquímica, Facultad de Ciencias Químicas, Universidad Complutense de Madrid, Avenida Complutense s/n, 28040 Madrid, Spain

<sup>c</sup>Networking Research Center on Bioengineering, Biomaterials and Nanomedicine (CIBER-BBN), Spain

† Electronic supplementary information (ESI) available: Reagents and equipment, X-ray powder diffraction pattern of the  $\gamma$ -Fe<sub>2</sub>O<sub>3</sub> NPs, selected characterization data for dendritic precursors (G1-G3), DLS measurement of G3-MNPs after months of storage. See DOI: 10.1039/c0jm03526b

have many biomedical applications, for instance, as contrast agents in magnetic resonance imaging, in drug delivery and in neutron capture and gene transfection therapies.<sup>14–16</sup> Regarding the latter, polyamidoamine (PAMAM) and poly(propyleneimine) (PPI) dendrimers, have been thoroughly studied recently as nonviral gene transfection agents,<sup>6,17,18</sup> especially for cancer therapy, overcoming the safety disadvantages of viral vector systems. These dendrimers form compact poly-cations under physiological conditions able to complex, transport and protect DNA.

It has been reported that mesoporous silica nanoparticles and gold nanoparticles modified with low generation  $-NH_2$  terminated dendrimers, such as the PAMAM and PPI dendrimers, display an effective gene transfection. Since a generation dependent cytotoxicity has been observed, this approach has the benefit of using non-toxic generations. Moreover, the drawback of the limited surface charges of low generation dendrimers is overcome *via* the attachment of several dendritic molecules to the same nanoparticle, which leads to an efficient DNA complexation.<sup>19,20</sup> A similar observation has been reported for systems that use different sizes of polyethyleneimine polymers attached to mesoporous silica nanoparticles.<sup>21</sup>

Different synthetic approaches for the functionalization of iron oxide nanoparticles with dendritic macromolecules have been developed for a variety of applications. For intracellular uptake studies iron oxide NPs have been stabilized with carboxylated poly(amidoamine) dendrimers through electrostatic self assembly onto the iron oxide surfaces.<sup>22–24</sup> Regarding catalytic applications, attempts to grow dendrimers directly on magnetic nanoparticles usually fail due to coagulation of the particles and solubility problems in organic media. To solve these problems the magnetic nanoparticles can be coated with silica.<sup>25</sup> Nevertheless, a stepwise growth of dendritic PAMAM wedges on the surface of magnetite NPs has been reported for gene delivery.<sup>26</sup> Another relevant approach is the modification of the iron oxide nanoparticles by combining the electrostatic layer by layer self assembly technique with dendrimer chemistry. Positively charged iron oxide NPs were modified with a bilayer composed of a negatively charged polyelectrolyte and a generation 5 PAMAM dendrimer.<sup>27</sup> In this sense, a more stable shell coating was obtained when iron oxide NPs were assembled with multilayers of polyelectrolytes and an outer layer of PAMAM dendrimers to finally carry out a chemical crosslinking of the shells.<sup>28</sup> By using dendrimers that bear folic acid as the targeting moiety these multifunctional iron oxide NPs were able to be used for targeting and imaging of cancer cells.

Herein, we describe a process to covalently graft PPI dendrimers onto the naked surface of maghemite nanoparticles ( $\gamma\text{-Fe}_2\text{O}_3$  NPs). The dendrimers are strongly anchored onto the iron oxide surface in one synthetic step, by exploiting the sol–gel approach to attach functional alkoxysilane derivatives to iron oxide NPs.<sup>29–32</sup> This method represents a new strategy to synthesize dendrimer functionalized magnetic nanoparticles that form stable colloidal solutions in water and facilitates potential biomedical applications of these magnetic nanoparticles. Our attractive methodology is less time consuming and keeps intact the structure of the dendrimer, *versus* the use of multistep procedures that lead to dendritic wedges or dendrons or, to a certain extent, to hyperbranched polymers. Statistically, when

using the divergent growth approach, only a small proportion of the higher generations of dendrimers can be perfect<sup>33,34</sup> and moreover, with the use of a solid support the steric interference effect would be pronounced.

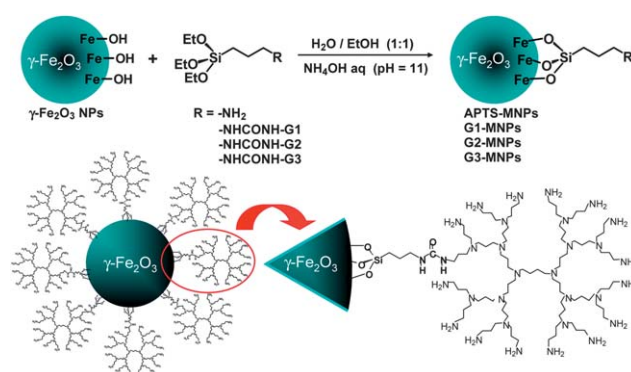
In this work we present a novel multifunctional nanosystem for *in vitro* gene transfection that consists of poly(propyleneimine) dendrimers covalently bonded to maghemite nanoparticles, as depicted in Scheme 1. On the one hand, PPI dendrimers can act as nonviral gene transfection agents<sup>6,35</sup> and provide complexation sites for effective DNA binding in the proposed nanovector. Moreover, the presence of tertiary amines protects the genes from the acid attack in the endosomal compartment. On the other hand, superparamagnetic iron oxide NPs would make magnetofection feasible, speeding up the gene transfection. It is noteworthy that the covalent bonding between the dendrimers and the magnetic nanoparticle ensures the vector integrity during the transfection process.

## Results and discussion

### A novel approach for the covalent assembly of PPI dendrimers to maghemite NPs

The magnetic NPs were prepared as maghemite ferrofluid according to the Massart method.<sup>36,37</sup> Controlled alkaline coprecipitation of  $\text{Fe}^{\text{II}}$  and  $\text{Fe}^{\text{III}}$  ions yields nanometric magnetite ( $\text{Fe}_3\text{O}_4$ ), which is subsequently oxidized to maghemite ( $\gamma\text{-Fe}_2\text{O}_3$ ). In this fashion continuous variation of the iron oxide cores from magnetite to maghemite is avoided.

The synthetic route followed for the covalent grafting of dendrimers to the  $\gamma\text{-Fe}_2\text{O}_3$  NPs is shown in Scheme 1. Our approach is based on the previous synthesis of the partially silylated dendritic precursors (Chart 1).<sup>38</sup> Reaction conditions of this step are optimized to get the monosubstituted dendrimers as the major product. Accordingly, one of the peripheral amino groups of the dendrimers, as an average, is used to introduce a reactive functional group, such as  $-\text{Si}(\text{OEt})_3$ , that allows covalent bonding to the  $\text{Fe}-\text{OH}$  groups on the surface of the magnetic nanoparticles (MNPs) in a subsequent step of synthesis.



**Scheme 1** Dendritic functionalization of iron oxide nanoparticles through sol–gel chemistry with alkoxysilane PPI dendrimers. Magnetic NPs functionalized with APTS (as a model), G1, G2 and G3 were prepared. Schematic structure of G3-MNPs material.

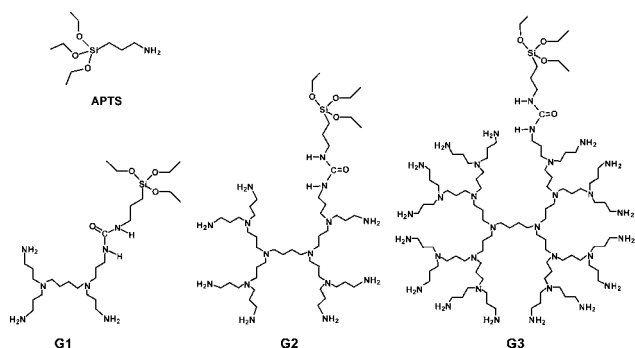


**Chart 1** 3-Aminopropyltriethoxysilane and schematic representation of dendritic precursors G1–G3.

The surface modification of  $\gamma$ -Fe<sub>2</sub>O<sub>3</sub> NPs was performed following a sol–gel based wet-chemistry synthetic route, under basic pH conditions.<sup>39</sup> In this way, the silanization reaction leads to the formation of core–shell hybrid structures, although under these conditions the self-condensation of alkoxy silane dendritic precursors in the presence of water cannot be avoided. Then, alkoxy silane auto condensation is produced, but it is hampered in the higher dendrimer generations due to steric hindrance. Nanosystems prepared with G3 dendrimers exhibit experimental organic amounts closer to theoretical values, when compared with G2, G1 or even with only APTS, as demonstrated by thermogravimetric and elemental analyses (Table 1). This means that the ratio of interdendrimer condensation *versus* condensation with the inorganic surface decreases as the dendrimer generation increases. This fact is explained in terms of steric hindrance between G3 dendrimers, avoiding the self-condensation of alkoxy silane dendritic precursors, thus favouring condensation with the maghemite nanoparticles.

In order to confirm the covalent anchoring of the dendrimers through the alkoxy silane moiety with the Fe–OH groups, we performed a parallel attempt to functionalize the  $\gamma$ -Fe<sub>2</sub>O<sub>3</sub> NPs with the third generation dendrimer lacking the triethoxysilane group. Moreover, this test was also useful to discard the coating of the MNPs through electrostatic interactions. The experiment,

**Table 1** Percentage of maghemite, experimental and theoretical organic material content, isoelectric point and hydrodynamic particle size of the magnetic nanoparticles

Material	% $\gamma$ -Fe <sub>2</sub> O <sub>3</sub>	% Org. Matter	% Org. Matter Theoretical	IEP	Particle Size (nm) <sup>a</sup>
$\gamma$ -Fe <sub>2</sub> O <sub>3</sub> NPs	100	0	0	7.1	8
APTS-MNPs	99.87	0.13	3.66	9.0	16
G1-MNPs	98.46	1.54	20.77	10.1	18
G2-MNPs	90.10	9.90	35.92	10.6	21
G3-MNPs	72.66	27.34	53.66	11.0	39
G3-MNPs <sup>b</sup>	94.27	5.73	52.45	N/A <sup>c</sup>	N/A <sup>c</sup>

<sup>a</sup> Maximum of the size distribution, measured by DLS in water (1–5 mg mL<sup>-1</sup>) at pH 3 (HNO<sub>3</sub>). <sup>b</sup>  $\gamma$ -Fe<sub>2</sub>O<sub>3</sub> NPs with G3 dendrimer lacking the triethoxysilane group. <sup>c</sup> Could not be measured due to high polydispersity.

carried out under identical experimental conditions, failed to yield stable and water soluble MNPs. The obtained sample was a non-homogeneous dispersion with aggregates and a high polydispersity, and behaved neither as the bare  $\gamma$ -Fe<sub>2</sub>O<sub>3</sub> NPs ferrofluid nor as the MNP-G3 particles. Thermogravimetric and chemical analyses gave a low organic content, indicating the loss of the unattached dendrimer with the magnetic washings (Table 1).

### Surface charge measurements

The surface modification of the  $\gamma$ -Fe<sub>2</sub>O<sub>3</sub> NPs was confirmed with the zeta ( $\zeta$ )-potential measurements of the functionalized MNPs colloidal aqueous solutions. The attachment of APTS or the PPI dendrimers to the  $\gamma$ -Fe<sub>2</sub>O<sub>3</sub> NPs surface provides an amino group density that decisively defines the MNPs surface charge along the pH range, *i.e.*, their zeta potential (Fig. 1.A). The bare iron oxide NPs have the isoelectric point (IEP) at neutral pH and it is shifted towards higher pH values after functionalization (Table 1).

As the generation of the grafted dendrimer increases there is an exponential increase in primary and tertiary amines of the dendrimer framework. This is reflected by the progressive shift in the IEP values, rising to *ca.* 11 for the third dendrimer generation. It is noteworthy that the  $\zeta$ -potential distributions at a given pH are monomodal for all materials, indicating single component samples and homogeneous surface coverage of the MNPs (Fig. 2.A). Furthermore, the  $\zeta$ -potential return titration curves of

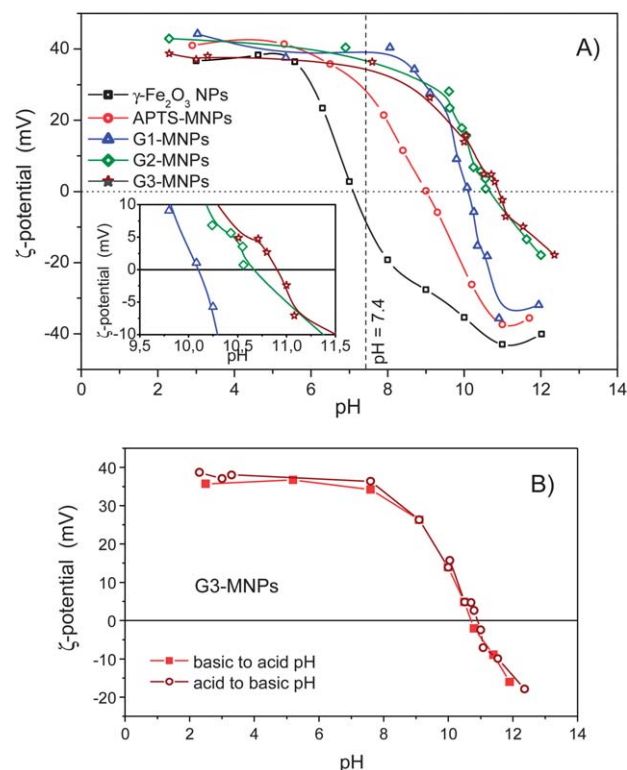


**Fig. 1** (A) Evolution of  $\zeta$ -potential curves as a function of pH for bare  $\gamma$ -Fe<sub>2</sub>O<sub>3</sub> NPs and APTS and dendrimer functionalized MNPs. Inset: magnification. (B) Evolution of  $\zeta$ -potential return titration curves as a function of pH for the third generation dendrimer functionalized MNPs.

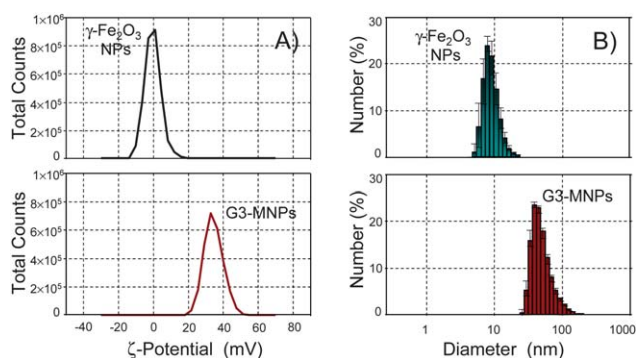


**Fig. 2** (A)  $\zeta$ -potential distributions at pH 7.1 (IEP of  $\gamma\text{-Fe}_2\text{O}_3$  NPs) for MNPs before and after functionalization with G3 dendrimer. (B) Hydrodynamic diameter distribution obtained by DLS for the bare  $\gamma\text{-Fe}_2\text{O}_3$  NPs and G3 dendrimer functionalized MNPs nanoparticles.

the dendrimer functionalized MNPs do not show any hysteresis, which indicates a high chemical stability of the dendrimer-iron oxide linkage through the siloxane linker and is consistent with covalently bonded dendrimers (Fig. 1.B). The IEP values, ranging from *ca.* 10 to 11, as well as the  $\zeta$ -potential value at pH 7.4, *ca.* +37 mV, for the dendrimer-MNPs represent a high positive charge at physiological pH. Therefore, aggregation or flocculation of the MNPs is avoided at pH 7.4 since the electrostatic stability of the colloidal ferrofluids is ensured.

### Hydrodynamic diameter measurements

The hydrodynamic mean diameter distributions of the functionalized MNPs obtained by dynamic light scattering (DLS) are monomodal and narrow for all materials (Fig. 2.B). It is evidenced by a sequential higher value, with the dendrimer generation grafted, that goes from 8 nm for the uncoated MNPs up to 39 nm for the third generation dendrimer functionalized MNP (Table 1). The existence of dendrimers with more than one silylated branch in the functionalizing solution is expected from the synthetic methodology and it has been characterized (see Electronic Supplementary Information†).<sup>38</sup> In such a case, condensation of the same dendritic molecule with a number of MNPs cannot be overruled and contributes to some extent to a MNPs aggregation process. This is shown by the asymmetry of the size distribution, which is shifted towards higher values for a low number of particles after dendrimer attachment (Fig. 2.B).

The dendrimer-MNPs showed excellent long-term colloidal stability in water solution, remaining indefinitely stable in water at pH = 7.4. The hydrodynamic diameter was monitored by DLS at different periods of time, remaining practically unchanged for months (ESI†). Such colloidal stability can be attributed to both steric and electrostatic repulsive forces, as expected from DLS and  $\zeta$ -potential measurements. Importantly, the covalent attachment of the dendrimer shell to the particle surface ensures that the dendritic surface function remains on the nanoparticle throughout storage time as well as during application.

Since dendrimer-MNPs nanosystems were designed to conduct biological experimentation, surface charge and hydrodynamic diameter of the G3-MNPs were also measured in cell culture media. Data show that G3-MNPs colloidal stability is preserved in media with a higher ionic strength such as DMEM,

since  $\zeta$ -potential at pH 7.4 still maintains a high positive value (28 mV). A lower particle size, equal to 34 nm, can be attributed to a backfolding of the end groups of PPI dendrimers that takes place at high salt concentration, giving rise to a dense core dendritic structure.<sup>40</sup> The shift to lower  $\zeta$ -potential values (5 mV) of the nanosystem in cell culture media supplemented with serum indicates serum protein adsorption onto the nanoparticles. Accordingly, bigger aggregates of *ca.* 53 nm are formed.<sup>11,21</sup>

### Magnetic measurements

The magnetic properties of the ferrofluid containing the MNPs functionalized with the third generation dendrimer were investigated by means of vibrating sample magnetometry. The magnetization curve normalized to the mass of  $\gamma\text{-Fe}_2\text{O}_3$  is displayed in Fig. 3, together with the measurement of the bare  $\gamma\text{-Fe}_2\text{O}_3$  NPs ferrofluid. The MNPs preserve their superparamagnetic properties after the covalent anchorage of the G3 dendrimer. This characteristic superparamagnetic behaviour is indicated by the absence of a hysteresis loop on the magnetization curve, *i.e.*, zero coercivity and zero remanence, measured at room temperature. Moreover, the initial slopes show a rapid approach to saturation, suggesting a high magnetic susceptibility. The saturation magnetization values are 58.44 and 50.93  $\text{emu g}^{-1}$  for the bare  $\gamma\text{-Fe}_2\text{O}_3$  NPs and the MNP-G3, respectively. These values are lower than that of bulk maghemite ( $76 \text{ emu g}^{-1}$ ), but comparable to results reported for similar size iron oxide NPs, ranging from 30 to 60  $\text{emu g}^{-1}$ .<sup>41,42</sup> The anchorage of the dendrimer to the iron oxide MNPs surface results in a decrease in the saturation magnetization. This fact is attributed to the covalent grafting of the dendrimers through siloxane bonds, which directly affects the crystallo-chemical properties of the MNPs surface and leads to an increase in the magnetically disordered surface layer.<sup>43</sup>

### Gene transfection experiments of DNA/G(1,2,3)-MNPs complexes

*In vitro* transfection efficiency of the materials was evaluated as a function of parameters such as dendrimer generation, different

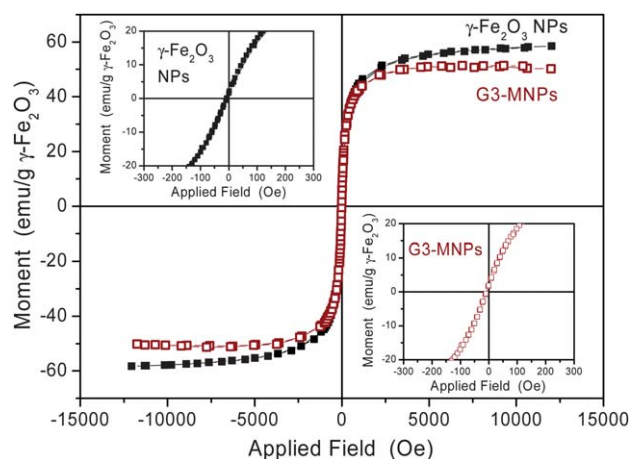


**Fig. 3** Magnetization curves at room temperature of the  $\gamma\text{-Fe}_2\text{O}_3$  NPs and G3-MNPs ferrofluids. The insets show an enlarged view near the origin.

plasmid/dendrimer-MNP weight ratios, incubation time and the presence or absence of the magnetic field. A plasmid DNA (pEGFP-N3) that codes for an enhanced green fluorescent protein (EGFP) was used as reporter gene. The highest transfection efficiency (*ca.* 12%), without cytotoxic reactions, was obtained with the third generation dendrimer (DNA/G3-MNPs) using a weight ratio of 1/5 and under magnetic stimulus. No improvement of the transfection efficiency was found for the DNA/G3-MNPs complex at weight ratios of 1/10 and 1/20. Considering that nonviral transfection on Saos-2 cells have been rarely reported and that studies with several commercial nonviral vectors showed, as the best result after optimization, comparable transfection efficiencies (*ca.* 13%),<sup>44</sup> this nanosystem can be considered an important contribution to the field.

Studies with DNA/G1-MNPs and DNA/G2-MNPs complexes demonstrate higher values of cell viability (98%) and lower values of apoptosis (1%). However very low transfection efficiency (<1%) was obtained with these complexes in the same conditions (Fig. 4.B).

These results could be explained in terms of the increasing amounts of primary and tertiary amine groups, insofar the dendrimer generation increases. At pH = 7.4 the peripheral primary amines ( $pK_a$  9–11) are positively charged ammonium groups, complexing the DNA fragment through ionic interaction with negatively charged phosphate groups of nucleic acids. The entry into the cell *via* endocytosis is optimized since protonated residues on the resulting compact complexes favours the binding to the negatively charged cell surface. Thereafter, the tertiary amines ( $pK_a$  5–8) of the dendrimer framework are responsible for a “proton sponge” behavior at the intracellular level. Their protonation protects the DNA from degradation in an endosomal compartment (pH 5–6). Both, DNA complexation for the endocytosis process and proton sponge behaviour, would explain the efficiency found with the third generation system.<sup>6,17,35</sup> Comparing the three dendritic generations attached to the MNPs, it is observed that gene transfection occurs when the amine content is higher than a threshold amine value, which is the case for the third generation nanosystem (see organic matter percentage, Table 1). The magnetic field was essential for the gene delivery in short periods of time. Exposure to the magnet for up to 20 min produced significant transfection efficiency, and no transfection was observed for the same delivery time in the absence of the magnetic field (Fig. 4).

The biocompatibility of DNA/G3-MNPs complex was evaluated by the analysis of cell viability and apoptosis by flow cytometry after magnetofection (Fig. 5.A). The results demonstrated that the treatment produced a slight decrease in viable

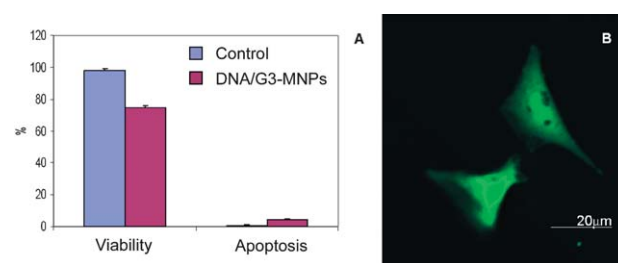


**Fig. 5** (A) Cell viability and apoptosis of osteoblasts after magnetofection with the DNA/G3-MNPs complex (1/5 weight ratio). (B) Fluorescence confocal micrographs of osteoblasts transfected by magnetofection with the DNA/G3-MNPs complex.

cells (25%) in comparison with control, but very low levels of apoptosis were detected (4%), thus indicating the absence of cytotoxicity of this material. Fig. 5.B shows the significant EGFP expression after osteoblast magnetofection with the DNA/G3-MNPs complex observed by confocal microscopy.

## Experimental

### Preparation of magnetic nanoparticles

Magnetic nanoparticles (MNPs) were prepared by controlled coprecipitation of  $Fe^{II}$  and  $Fe^{III}$  ions and subsequent oxidation, resulting in a nanometric maghemite ( $\gamma-Fe_2O_3$ ) containing-ferrofluid.<sup>29,36,37</sup> Briefly,  $NH_4OH$  (75 mL, 30% wt.) was added under vigorous stirring to an aqueous solution of ferric chloride (875 mL, 21.51 g  $FeCl_3 \cdot 6H_2O$ ) and ferrous chloride (42.5 mL HCl 1.5 M, 7.83 g  $FeCl_2 \cdot 4H_2O$ ) to obtain a black precipitate. The precipitate was magnetically decanted and the particles were oxidized to maghemite ( $\gamma-Fe_2O_3$ ) by the addition of a solution of iron nitrate (150 mL, 20.41 g  $Fe(NO_3)_3 \cdot 9H_2O$ ) and heating at 90 °C for 30 min. After that, the product was washed with acetone several times, and finally dispersed in water/ $HNO_3$  at pH 3 to a concentration of 311 mg  $mL^{-1}$ . The ferrofluid so-obtained was composed of magnetic nanoparticles with an average diameter of 8 nm at pH 3, as measured by dynamic light scattering. The isoelectric point of the resulting ferrofluid occurs at neutral pH ( $pH = 7.1$ ), as derived from  $\zeta$ -potential results. Magnetic measurements from this ferrofluid are characteristic of a superparamagnetic material since no hysteresis loop is displayed, and saturation magnetization is equal to 58  $emu\ g^{-1}$  (62  $emu\ g^{-1}$  for the dry powdered nanoparticles). Specific surface area of the dry powdered sample measured by nitrogen adsorption analysis was 140  $m^2\ g^{-1}$ .

### Synthesis of silylated dendrimers G1–G3

Alkoxysilane partial functionalization of the first, second and third generation of poly(propyleneimine) dendrimers,  $DAB(NH_2)_x$  ( $x = 4, 8, 16$ ), was carried out.<sup>38</sup> As an example, the synthesis of G3 is described: Under an inert atmosphere of  $N_2$  a solution of 3-isocyanatopropyltriethoxysilane (0.0809 g, 82  $\mu L$ , 0.327 mmol) in dry  $CH_2Cl_2$  (45 mL) was added dropwise (over a 3 h period of time) to a rapidly stirred solution of  $DAB-3-(NH_2)_{16}$  (0.5516 g, 0.327 mmol) in dry  $CH_2Cl_2$  (45 mL). The reaction mixture was stirred overnight at room temperature and

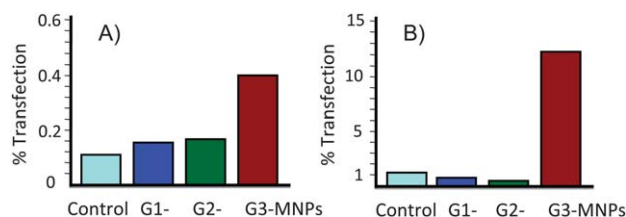


**Fig. 4** Transfection efficiencies for the DNA/G(1,2,3)-MNP complexes (1/5 weight ratio) for 20 min of incubation time (A) without magnetic stimulus and (B) under magnetic stimulus.

then filtered off (under an inert atmosphere). To this solution EtOH was added and  $\text{CH}_2\text{Cl}_2$  removal under vacuum afforded the dendritic precursor dissolved in 100 mL of EtOH, ready to be immediately used in the next step.

### Attachment of dendrimers onto the iron oxide nanoparticles surface

The amount of alkoxy silane derivative required to functionalize 0.50 g of MNPs was calculated to achieve a maximum surface coverage, *i.e.*, a 100% nominal degree of surface functionalization. Therefore, it was taken into account the specific surface area of the isolated powder materials, an average surface concentration of Fe–OH groups in  $\gamma\text{-Fe}_2\text{O}_3$  of 14  $\mu\text{mol}$  –OH per  $\text{m}^2$ <sup>29</sup> and the stoichiometry of three Fe–OH groups with one dendritic molecule or  $-\text{Si}(\text{OEt})_3$ .

The surface modification of  $\gamma\text{-Fe}_2\text{O}_3$  NPs was performed following a sol–gel based wet-chemistry synthetic route, under basic pH conditions.<sup>30,39</sup> The functionalization is performed at pH = 11, far enough off the IEP of the bare  $\gamma\text{-Fe}_2\text{O}_3$ , so the surface chemical reactions are performed on isolated NPs not on flocculates.

A solution of the calculated amount of alkoxy silane derivative (APTS, G1, G2 or G3) in 100 mL of EtOH was added under stirring to 100 mL of the maghemite ferrofluid containing 0.5 g of MNPs. The pH value was set to 11.0 with ammonia solution 30% wt and the reaction was then placed in an ultrasonic bath for 5 h ( $T = ca.$  50 °C). The resulting MNPs were thoroughly washed with EtOH–H<sub>2</sub>O and water, assisted by magnetic separation, to remove any non-covalently bound and unbound organic molecules (silylated or non-silylated dendrimers), and finally left in aqueous media (pH = 3, HNO<sub>3</sub>) as colloidal solutions. Prior to the *in vitro* transfection experiments the pH of the colloidal dendrimer-MNPs solutions was adjusted to 7.4, and the iron content of the resulting ferrofluids was determined by atomic emission spectroscopy.

Dendrimer-MNPs colloidal solutions were characterized by means of atomic emission spectroscopy, magnetic measurements, dynamic light scattering and zeta-potential measurements. Dry samples for solid state characterization (XRD, TGA, DTA, chemical microanalysis and FTIR) were prepared by extensive dialysis against water and subsequently dried and grounded. Remarkably, G3 functionalized MNPs show excellent water solubility after drying.

### Cell culture for magnetofection studies

Human Saos-2 osteoblasts were maintained in T75 flasks using DMEM (Dulbecco's modified Eagle's medium) supplemented with 10% heat-inactivated fetal bovine serum (FBS, Gibco, BRL), 1 mM L-glutamine (BioWhittaker Europe, Belgium), penicillin (200  $\mu\text{g mL}^{-1}$ , BioWhittaker Europe, Belgium), and streptomycin (200  $\mu\text{g mL}^{-1}$ , BioWhittaker Europe, Belgium), under a CO<sub>2</sub> (5%) atmosphere at 37 °C. All cells were passaged every 3 days.

A red-shifted variant of GFP expressed from pEGFP-N3 (Clontech, Palo Alto, CA) was used as reporter protein. All plasmids were amplified in the *E. coli* strain DH5 $\alpha$  and purified according to the manufacturer's protocol (Qiagen, USA). The

isolated DNA was resuspended in Tris-EDTA (pH 8.0) at a concentration of 1  $\mu\text{g mL}^{-1}$ .

Human Saos-2 osteoblasts were used for magnetofection test. Saos-2 were seeded on 6 well culture plates (CULTEK S.L.U., Madrid, Spain, reference 153516, growth surface of 11  $\text{cm}^2/\text{well}$ ), at a density of 10<sup>5</sup> cells/well, in 2 mL growth medium at 37 °C for 24 h prior to the experiment. Cells were approximately 50% confluent at the time of transfection.

The complexes were prepared by gently mixing 1  $\mu\text{g}$  of pEGFP and G1-MNPs, G2-MNPs and G3-MNPs materials at weight ratios of 1/2.5, 1/5, 1/10 and 1/20 in Tris-EDTA buffer. The complex mixtures were incubated 30 min at RT. An equal volume of OptiMEM-1 medium (CE, Invitrogen S A, Spain) was added to these DNA/G1-MNPs, DNA/G2-MNPs and DNA/G3-MNPs complex solutions which were incubated for another 30 min at RT. Cells were washed three times with Phosphate Buffer Saline (PBS) and 1.4 mL OptiMEM-1 were added by well. Then, 100  $\mu\text{L}$  of each DNA/G(1,2,3)-MNPs complex solution were added to the cultures resulting in a final volume of 1.5 mL.

In a typical magnetofection experiment, the cell culture plate was placed upon the magnetic plate for 20 min. After that, the transfection mixture containing residual DNA/G(1,2,3)-MNPs complexes was removed and the transfected cells were cultured for 2 days with DMEM supplemented with 10% calf serum and antibiotics in order to evaluate the enhanced green fluorescent protein (EGFP) expression by flow cytometry and confocal microscopy. Controls either in the absence or presence of G(1,2,3)-MNPs materials or pEGFP plasmid were carried out. Also, control transfection experiments with Escort IV Transfection Reagent (Sigma, non-magnetic vector) were carried out obtaining 17% transfection efficiency after 6 h of delivery time.

### Analysis of biocompatibility and transfection efficiency of G(1,2,3)-MNPs by flow cytometry

In order to evaluate the percentage of transfected osteoblasts and the material biocompatibility, the medium was aspirated after magnetofection and the cells were washed with PBS and harvested using 0.25% trypsin-EDTA solution. After 15 min, the reaction was stopped with culture medium and the cells were then centrifuged at 310  $\times g$  for 10 min and resuspended in fresh medium for the analysis of EGFP expression, cell viability and apoptosis by flow cytometry. The number of transfected cells was obtained by the EGFP fluorescence analysis in a FacScalibur Becton Dickinson flow cytometer. Cell viability was determined by addition of propidium iodide (PI; 0.005% in PBS, Sigma-Aldrich Corporation, St. Louis, MO, USA) to stain the DNA of dead cells. The SubG<sub>1</sub> fraction of the cell cycle, used as indicative of apoptosis, was evaluated by incubation of cells with Hoechst 33258 (PolySciences, Inc., Warrington, PA, USA) (Hoechst 5  $\mu\text{g mL}^{-1}$ , ethanol 30%, and BSA 1% in PBS) for 30 min at room temperature in darkness. The fluorescence of Hoechst was excited at 350 nm and the emitted fluorescence was measured at 450 nm in an LSR Becton Dickinson flow cytometer. Each experiment was carried out three times and single representative experiments are displayed. For statistical significance, at least 10 000 cells were analyzed in each sample and the mean of the fluorescences emitted by these single cells was used.

## Detection of transfected cells by confocal microscopy

In order to observe the transfected osteoblasts after magnetofection, cells were examined by a Biorad MC1025 Confocal Laser Scanning Microscope. The fluorescence of EGFP was excited at 488 nm and the emitted fluorescence was measured at 530/30 nm. Cell viability was determined by addition of propidium iodide (PI; 0.005% in PBS, Sigma-Aldrich Corporation, St. Louis, MO, USA) to stain the DNA of dead cells.

## Conclusions

In this article we present a novel nonviral vector designed for DNA magnetofection based on PPI dendrimers and magnetic nanoparticles. The dendrimers are attached to the nanoparticles in one synthetic step, without any additional modification of the iron oxide surface. The nanosystem is chemically designed with a covalent bond between both components, thus ensuring the vector stability from the extracellular environment up to the cell interior. This strategy provides an important advantage, especially as a genetic engineering tool since DNA can be delivered in a short time while keeping the structure integrity. The transfection efficiency depends on the capability of the dendrimer generation to protect and transport the new gene into the nucleus.

## Acknowledgements

This work was supported by the Spanish CICYT through the project MAT2008-00736 and by the CAM through project S2009/MAT-1472. We thank C. Aroca and M. Maicas (ISOM, Universidad Politécnica de Madrid) for their technical assistance in the magnetic measurements.

## Notes and references

- 1 A. L. Feldman and S. K. Libutti, *Cancer*, 2000, **89**, 1181–1194.
- 2 K. Mancuso, W. W. Hauswirth, Q. Li, T. B. Connor, J. A. Kuchenbecker, M. C. Mauck, J. Neitz and M. Neitz, *Nature*, 2009, **461**, 784–787.
- 3 N. L. Rosi, D. A. Giljohann, C. S. Thaxton, A. K. R. Lytton-Jean, M. S. Han and C. A. Mirkin, *Science*, 2006, **312**, 1027–1030.
- 4 M. Selbach, B. Schwanhäusser, N. Thierfelder, Z. Fang, R. Khanin and N. Rajewsky, *Nature*, 2008, **455**, 58–63.
- 5 J. Dennig and E. Duncan, *Rev. Mol. Biotechnol.*, 2002, **90**, 339–347.
- 6 M. A. Mintzer and E. E. Simanek, *Chem. Rev.*, 2009, **109**, 259–302.
- 7 V. Sokolova and M. Eppele, *Angew. Chem., Int. Ed.*, 2008, **47**, 1382–1395.
- 8 D. Lechardeur, A. S. Verkman and G. L. Lukacs, *Adv. Drug Delivery Rev.*, 2005, **57**, 755–767.
- 9 F. Scherer, M. Anton, U. Schillinger, J. Henke, C. Bergemann, A. Krüger, B. Gänsbacher and C. Plank, *Gene Ther.*, 2002, **9**, 102–109.
- 10 B. Steitz, H. Hofmann, S. W. Kamau, P. O. Hassa, M. O. Hottiger, B. von Rechenberg, M. Hofmann-Antenbrink and A. Petri-Fink, *J. Magn. Magn. Mater.*, 2007, **311**, 300–305.
- 11 M. Arsianti, M. Lim, C. P. Marquis and R. Amal, *Langmuir*, 2010, **26**, 7314–7326.
- 12 R. Namgung, K. Singha, M. K. Yu, S. Jon, Y. S. Kim, Y. Ahn, I.-K. Park and W. J. Kim, *Biomaterials*, 2010, **31**, 4204–4213.
- 13 *Dendrimer Chemistry: Concepts, Synthesis, Properties, Applications*, ed. F. Vögtle, G. Richardt and N. Werner, Wiley-VCH, Weinheim, Germany, 2009.
- 14 D. Astruc, E. Boisselier and C. Ornelas, *Chem. Rev.*, 2010, **110**, 1857–1959.
- 15 R. K. Tekade, P. V. Kumar and N. K. Jain, *Chem. Rev.*, 2009, **109**, 49–87.
- 16 S. Svenson and D. A. Tomalia, *Adv. Drug Delivery Rev.*, 2005, **57**, 2106–2129.
- 17 C. Dufès, I. F. Uchegbu and A. G. Schätzlein, *Adv. Drug Delivery Rev.*, 2005, **57**, 2177–2202.
- 18 S.-F. Peng, C.-J. Su, M.-C. Wei, C.-Y. Chen, Z.-X. Liao, P.-W. Lee, H.-L. Chen and H.-W. Sung, *Biomaterials*, 2010, **31**, 5660–5670.
- 19 D. R. Radu, C. Y. Lai, K. Jeftinija, E. W. Rowe, S. Jeftinija and V. S.-Y. Lin, *J. Am. Chem. Soc.*, 2004, **126**, 13216–13217.
- 20 A. M. Chen, O. Taratula, D. Wei, H.-I. Yen, T. Thomas, T. J. Thomas, T. Minko and H. He, *ACS Nano*, 2010, **4**, 3679–3688.
- 21 T. Xia, M. Kovochich, M. Liong, H. Meng, S. Kabehie, S. George, J. I. Zink and A. E. Nel, *ACS Nano*, 2009, **3**, 3273–3286.
- 22 E. Strable, J. W. M. Bulte, B. Moskowitz, K. Vivekanandan, M. Allen and T. Douglas, *Chem. Mater.*, 2001, **13**, 2201–2209.
- 23 J. W. M. Bulte, T. Douglas, B. Witwer, S.-C. Zhang, E. Strable, B. K. Lewis, H. Zywicke, B. Miller, P. van Gelderen, B. M. Moskowitz, I. D. Duncan and J. A. Frank, *Nat. Biotechnol.*, 2001, **19**, 1141–1147.
- 24 X. Shi, T. P. Thomas, L. A. Myc, A. Kotlyar and J. R. Baker Jr., *Phys. Chem. Chem. Phys.*, 2007, **9**, 5712–5720.
- 25 R. Abu-Reziq, H. Alper, D. Wang and M. L. Post, *J. Am. Chem. Soc.*, 2006, **128**, 5279–5282.
- 26 B. Pan, D. Cui, Y. Sheng, C. Ozkan, F. Gao, R. He, Q. Li, P. Xu and T. Huang, *Cancer Res.*, 2007, **67**, 8156–8163.
- 27 S. H. Wang, X. Shi, M. Van Antwerp, Z. Cao, S. D. Swanson, X. Bi and J. R. Baker Jr., *Adv. Funct. Mater.*, 2007, **17**, 3043–3050.
- 28 X. Shi, S. H. Wang, S. D. Swanson, S. Ge, Z. Cao, M. E. Van Antwerp, K. J. Landmark and J. R. Baker Jr., *Adv. Mater.*, 2008, **20**, 1671–1678.
- 29 C. Flesch, M. Joubert, E. Bourgeat-Lami, S. Mornet, E. Duguet, C. Delaite and P. Dumas, *Colloids Surf., A*, 2005, **262**, 150–157.
- 30 S. Campelj, D. Makovec and M. Drogenik, *J. Magn. Magn. Mater.*, 2009, **321**, 1346–1350.
- 31 B. Srinivasan and X. Huang, *Chirality*, 2008, **20**, 265–277.
- 32 A. López-Cruz, C. Barrera, V. L. Calero-DdelC and C. Rinaldi, *J. Mater. Chem.*, 2009, **19**, 6870–6876.
- 33 D. A. Tomalia, A. M. Naylor and W. A. Goddard III, *Angew. Chem., Int. Ed. Engl.*, 1990, **29**, 138–175.
- 34 A. W. Bosman, H. M. Janssen and E. W. Meijer, *Chem. Rev.*, 1999, **99**, 1665–1688.
- 35 B. H. Zinselmeyer, S. P. Mackay, A. G. Schätzlein and I. F. Uchegbu, *Pharm. Res.*, 2002, **19**, 960–967.
- 36 R. Massart, *IEEE Trans. Magn.*, 1981, **17**, 1247–1248.
- 37 E. Ruiz-Hernández, A. López-Noriega, D. Arcos, I. Izquierdo-Barba, O. Terasaki and M. Vallet-Regí, *Chem. Mater.*, 2007, **19**, 3455–3463.
- 38 B. González, M. Colilla, C. López de Laorden and M. Vallet-Regí, *J. Mater. Chem.*, 2009, **19**, 9012–9024.
- 39 W. Stöber, A. Fink and E. Bohn, *J. Colloid Interface Sci.*, 1968, **26**, 62–69.
- 40 P. Welch and M. Muthukumar, *Macromolecules*, 1998, **31**, 5892–5897.
- 41 F. Montagne, O. Mondain-Monval, C. Pichot, H. Mozzanega and A. Elaissari, *J. Magn. Magn. Mater.*, 2002, **250**, 302–312.
- 42 A. Millan, A. Urtizberea, N. J. O. Silva, F. Palacio, V. S. Amaral, E. Snoeck and V. Serin, *J. Magn. Magn. Mater.*, 2007, **312**, L5–L9.
- 43 A.-H. Lu, E. L. Salabas and F. Schüth, *Angew. Chem., Int. Ed.*, 2007, **46**, 1222–1244.
- 44 P. Orth, A. Weimer, G. Kaul, D. Kohn, M. Cucchiarini and H. Madry, *Mol. Biotechnol.*, 2008, **38**, 137–144.